



Magnetic order in $\text{Tb}_2\text{Sn}_2\text{O}_7$ under high pressure: From ordered spin ice to spin liquid and antiferromagnetic order

I. Mirebeau,¹ I. Goncharenko,¹ H. Cao,¹ and A. Forget²

¹Laboratoire Léon Brillouin, CEA-CNRS, CE-Saclay, 91191 Gif-sur-Yvette, France

²Service de Physique de l'Etat Condensé, CEA-CNRS, CE-Saclay, 91191 Gif-sur-Yvette, France

(Received 19 November 2009; published 14 December 2009)

We have studied the $\text{Tb}_2\text{Sn}_2\text{O}_7$ ordered spin ice by neutron diffraction under an isotropic pressure of 4.6 GPa, combined with a stress of 0.3(1) GPa. Measurements down to a temperature of 0.06 K and up to 100 K probe the effect of pressure both on ground state and spin fluctuation in the paramagnetic region. In the pressure-induced ground state, the ordered spin ice structure with a $\mathbf{k}_0=0$ propagation vector persists, but it coexists with a structure with $\mathbf{k}_1=(0,0,1)$. The ordered moment at 0.06 K is reduced, suggesting that pressure also enhances the spin liquid fluctuations at $T\sim 0$. In the paramagnetic region, applying pressure changes the short-range spin correlations and suppresses the ferromagnetic correlations. The influence of pressure is discussed considering both isotropic pressure and stress effects.

DOI: [10.1103/PhysRevB.80.220407](https://doi.org/10.1103/PhysRevB.80.220407)

PACS number(s): 75.25.+z, 71.27.+a, 61.05.fm, 62.50.-p

Geometrical frustration combined with spin-lattice coupling is one of the key ingredients of physics, allowing one to design materials or tune several physical properties concomitantly. This cocktail is at play in some multiferroic and frustrated materials where electric, elastic, and magnetic order parameters interfere. In the ordered magnetic state, it may induce magnetoisostuctural transitions,¹ hybrid spin-lattice excitations,² and spontaneous distortions to remove the frustration like in the spin Peierls orders found in spinels.³ In the paramagnetic state, the interaction of the localized magnetic moments with a magnetic field may shift the ions from their equilibrium position, resulting in magnetostriction effects. Magnetoelastic coupling may also be probed by varying interatomic distances through pressure or stress and studying their effect on the magnetic properties.

Magnetoelastic coupling has also been recently invoked in the frustrated magnets called spin ices, whose magnetic short-range ordered ground state can be mapped to that of real ice⁴ and possesses the same entropy.⁵ In pyrochlore spin ices $R_2\text{Ti}_2\text{O}_7$ ($R=\text{Dy}, \text{Ho}$), the effective ferromagnetic (F) interactions between rare-earth R moments is combined with a strong uniaxial anisotropy, constraining the R moments along local $\langle 111 \rangle$ axes. Spin ices are presently highly topical, as their local magnetic structure supports excitations of magnetic monopoles,^{6,7} searched for decades, but never observed up to now. In spin ices, interesting spin-lattice coupling effects are expected.^{6,8} An isotropic pressure should tune the charge of the monopoles (inversely proportional to the interatomic distance) and their density since the energy to create a monopole varies with the strength of the exchange interaction, which depends on interatomic distances. Applying a stress may also suppress the spin ice state and induce a long-range order (LRO). But such effects have not been observed yet, and the influence of pressure or stress on spin ice magnetism seems to be very small (if there is any).^{9,10} Actually the strong anisotropy of the spin ices, where the ground-state crystal-field level of the R ion is far from the excited levels, results in a moderate magnetostriction.

In the $R_2\text{Ti}_2\text{O}_7$ family, the uniaxial anisotropy is much weaker for Tb than for Ho or Dy spin ices due to the peculiar

Tb crystal-field scheme, with an excited doublet separated from the ground-state doublet by a small gap of 10–20 K.^{11,12} This reduced anisotropy explains the giant magnetostriction¹³ of $\text{Tb}_2\text{Ti}_2\text{O}_7$ (TTO), and allows one to alter its spin liquid (SL) ground state by pressure and stress, inducing antiferromagnetic (AF) order.^{14,15} The effective Tb-Tb exchange interaction and the magnetic ground state may also be tuned by substituting Ti for Sn with larger ionic radius, which induces a lattice expansion.

$\text{Tb}_2\text{Sn}_2\text{O}_7$ (TSO) is an intriguing example of a soft or ordered spin ice, showing a local spin ice structure but long-range magnetic order and nonzero magnetization below ~ 1 K.¹⁶ The nature of this LRO and its coexistence with spin fluctuations in the ground state are highly debated.^{17–19} As outlined in the model of Champion *et al.*,²⁰ the weaker anisotropy of a soft spin ice yields an extra degree of freedom, the ratio of anisotropy and exchange energies, or equivalently the canting angle with respect to the $\langle 111 \rangle$ local trigonal axis, making it the “missing link” between true spin ice and Heisenberg ferromagnet. A soft spin ice should then be sensitive to changes in interatomic distances, both in paramagnetic and ordered regimes. In $\text{Tb}_2\text{Sn}_2\text{O}_7$, pressure or stress should affect both the local Tb environment through the crystal field and the Tb-Tb interactions in the geometrically frustrated lattice. Two scenarios could be *a priori* predicted for the effect of pressure on the spin correlations: (i) a “melting” of the spin ice long-range order, due to the decrease in the lattice constant, yielding a spin liquid state as in $\text{Tb}_2\text{Ti}_2\text{O}_7$ at ambient pressure and (ii) the onset of another ordered structure induced by a stress.

The best way to check such effects is to perform high-pressure neutron diffraction. Such a measurement is an experimental challenge, needing to combine high-pressure and very-low-temperature environments, with a sample volume several orders of magnitudes smaller than for usual powder neutron diffraction. Here, we report measurements of TSO under pressure. We studied the pressure-induced state both in the paramagnetic region up to 100 K and in the ordered spin ice region down to 0.06 K. By combining a high isostatic pressure of 4.6 GPa with a uniaxial stress of 0.3(1) GPa, we

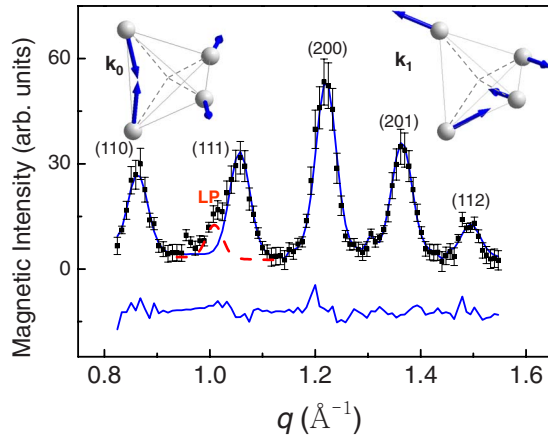


FIG. 1. (Color online) Magnetic diffraction pattern in $\text{Tb}_2\text{Sn}_2\text{O}_7$ at 0.06 K under a pressure of 4.6 GPa ($P_u \sim 0.4$ GPa). A spectrum at 4.5 K was subtracted. The solid line is a refinement involving \mathbf{k}_0 and \mathbf{k}_1 structures. Top: spin structures in one tetrahedron, having propagation vectors \mathbf{k}_0 (left) and \mathbf{k}_1 (right). The local anisotropy axes are in dashed lines.

find that the ordered spin ice structure with a $\mathbf{k}_0=0$ propagation vector partly transforms into a structure with $\mathbf{k}_1=(0,0,1)$, which has no net magnetization. Both structures coexist in the ground state. The LRO moment at 0.06 K is reduced with respect to its ambient pressure value, suggesting that the spin liquid ground state is favored by pressure. In the paramagnetic region, short-range order (SRO) between Tb moments is also affected by pressure.

A $\text{Tb}_2\text{Sn}_2\text{O}_7$ powder sample was inserted into a sapphire anvil cell, with an isostatic pressure component $P_i=4.6(1)$ GPa. High-pressure neutron-diffraction patterns were recorded at the diffractometer G6-1 of the Laboratoire Léon Brillouin,²¹ with an incident neutron wavelength $\lambda=4.74$ Å. Two experimental setups were used. In one setup, the sample was mixed with a pressure transmitting medium (40 vol % NaCl), yielding a uniaxial component $P_u \sim 0.2$ GPa along the axis of the pressure cell. The cell was inserted in a helium cryostat and diffraction patterns were recorded between 100 and 1.5 K to measure the SRO. Patterns were also recorded at ambient pressure on G6-1 and G4-1 ($\lambda=2.426$ Å) spectrometers for comparison. In the other setup, no transmitting medium was used to maximize the sample volume and increase P_u to ~ 0.4 GPa. Pressure components were measured by ruby fluorescence technique and through the positions of the NaCl Bragg peaks. The cell was fixed on the dilution insert of a cryostat, and diffraction patterns recorded between 0.06 and 4.5 K to measure the LRO. Magnetic patterns were obtained by subtracting a pattern measured at 100 and 4.5 K for SRO and LRO, respectively. The ordered Tb moments were calibrated by measuring the intensity of the (222) nuclear peak.

The magnetic pattern of $\text{Tb}_2\text{Sn}_2\text{O}_7$ in the pressure-induced ground state ($T=0.06$ K) shows the coexistence of two families of Bragg peaks indexed in the cubic unit cell of $Fd\bar{3}m$ symmetry (Fig. 1): those of the face-centered cubic lattice, with a propagation vector $\mathbf{k}_0=0$ which already exist at ambient pressure, and those of the simple cubic lattice,

indexed by a vector $\mathbf{k}_1=(0,0,1)$, which appear under pressure. A small peak also appears under pressure at $q=1.01$ Å⁻¹. It is attributed to a long period structure with a larger unit cell than the cubic one, which cannot be characterized. The magnetic structures corresponding to the two families were analyzed separately since they do not yield Bragg reflections at the same positions. The intensities of the overlapping $q=1.01$ Å⁻¹ and (111) peaks were determined by fitting them to Gaussian lines.

The \mathbf{k}_0 structure, similar to that found at ambient pressure,¹⁶ has four identical tetrahedra in the cubic cell. It is one of the possible structures allowed by the crystal symmetry found by means of representation analysis²² in the space group $I4_1/amd$, the largest subgroup of the $Fd\bar{3}m$ space group allowing a ferromagnetic component. The local spin structure in a tetrahedron (Fig. 1, top left) is simply described by the ordered Tb moment M_0 (the same for all Tb ions, determined by absolute calibration) and its canting angle α with respect to the $\langle 111 \rangle$ local anisotropy axis. The refinement at 0.06 K ($R=1\%$) yields $M_0=3.3(3)\mu_B$ and $\alpha=28(1)^\circ$ to be compared with the ambient pressure values $M_0=5.9(1)\mu_B$ and $\alpha=13^\circ$. So, under pressure the Tb moments in the $\mathbf{k}=0$ structure decrease and turn away from their local easy axis. The magnetization evaluated to $2.2\mu_B/\text{Tb}$ at 1 bar is reduced to $0.4(1)\mu_B$ under pressure.

In the \mathbf{k}_1 structure, two tetrahedra of the cubic unit cell have identical orientations of the magnetic moments, and two tetrahedra have reversed orientations. This structure has no ferromagnetic component. It is somewhat similar to that found in TTO under pressure. The details of its local spin structure inside a tetrahedron remain unknown since several configurations refine the data equally well. A possible spin structure ($R=3\%$) is given in Fig. 1 (top right). From our analysis, we outline two robust characters of the local structure, namely, the average Tb moment in a tetrahedron, which keeps a value $M_1=2.7(2)\mu_B$ at 0.06 K, and the presence of an antiferromagnetic pair of Tb moments.

By measuring the temperature dependence of the magnetic Bragg peaks [Fig. 2(a)], we can determine the transition temperature. As for the \mathbf{k}_0 structure, the value $T_0=1.2(1)$ K is close to the upper transition in TSO at ambient pressure which situates at $1.3(1)$ K. At ambient pressure, the order parameter (inset in Fig. 2) shows a steep variation at the lower transition of 0.87 K. The first-order character of the transition is also supported by a small anomaly of the lattice constant [Fig. 2(b)]. Under pressure, the T dependence of the magnetic intensity is strongly smeared, without any anomaly. The \mathbf{k}_1 structure collapses at a slightly higher temperature $T_1=1.6(1)$ K.

We now discuss the influence of pressure on the SRO, measured just above the transition. Difference patterns at 1.5 K with respect to 100 K clearly show broad modulations of the intensity I_{SRO} versus the momentum transfer [Fig. 3(a)], which change under pressure [Fig. 3(b)]. At ambient pressure, I_{SRO} was fitted by the expression $I_{\text{SRO}}=F^2(q)[I(q)+L(q)]+C$, where $F(q)$ is the magnetic form factor of the Tb^{3+} ion, $L(q)$ is a Lorentzian function, and C a constant background. The liquidlike function $I(q)=\gamma_1 \sin(qR_1)/(qR_1)$ accounts for correlations between first-neighbor Tb

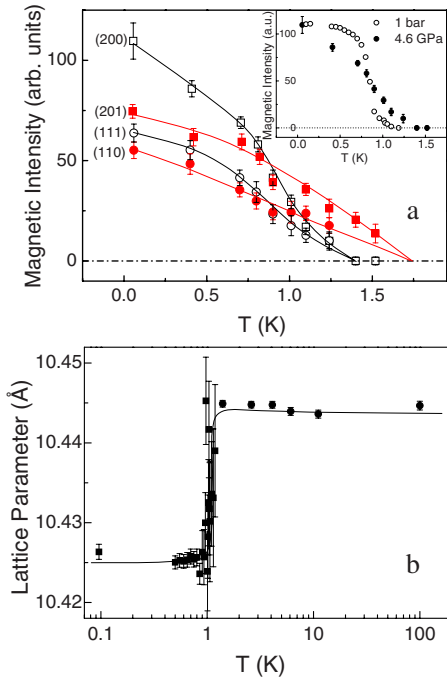


FIG. 2. (Color online) (a) integrated intensity of the F (\square , \circ) and AF (\blacksquare , \bullet) peaks versus temperature under pressure ($P_i=4.6$ GPa, $P_u=0.4$ GPa). Lines are guides for the eye. Inset: (200) peak intensities with and without pressure, scaled at 0.06 K. (b) Temperature dependence of the lattice constant at ambient pressure.

pairs at a distance R_1 . It has two maxima in the measured q range, as also seen in TTO.²³ The γ_1 value is negative, showing that first-neighbor Tb pairs are AF coupled, and its increase in modulus on cooling (Fig. 4) reflects the increasing correlations as the temperature decreases. The Lorentzian term $L(q)$ accounts for ferromagnetic correlations, expected just above the ordered spin ice transition, and still observed below. It enhances the magnetic intensity at low q 's, shifts the position, and damps the intensity of the two maxima. Under pressure, the γ_1 value remains unchanged, whereas the Lorentzian term vanishes [Fig. 3(b)]. The fit of the SRO under pressure is slightly improved by inserting third-neighbor correlations between Tb moments (with ferromagnetic γ_3), noticing that second-neighbor Tb pairs are absent in the pyrochlore structure. The suppression of the Lorentzian term by pressure suggests that the critical fluctuations associated with the ordered spin ice transition vanish, as the \mathbf{k}_1 structure is stabilized.

The nature of the pressure-induced ground state may be understood by referring both to TSO at ambient pressure and TTO under pressure and stress. At 0.06 K the ordered moment M per Tb ion, considering both F and AF structures, can be calculated as $M^2=M_0^2+M_1^2$, yielding $M=4.3(3)\mu_B$. Taking into account the long period structure, one gets a value of $4.5(3)\mu_B$. So, the pressure-induced ordered moment is strongly reduced with respect to the ambient pressure value of $5.9(1)\mu_B$. We attribute this effect to the enhancement of the spin liquid fluctuations, which should naturally wash out the magnetic long-range order.

We therefore conclude that the applied pressure favors

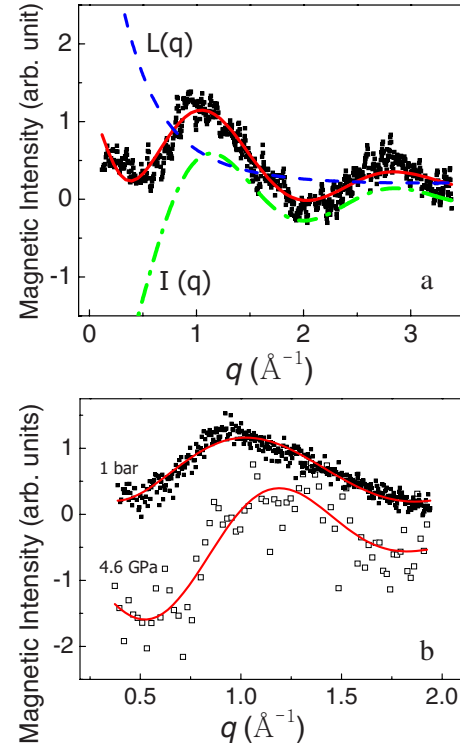


FIG. 3. (Color online) Magnetic SRO patterns at 1.5 K; a pattern at 100 K was subtracted. (a) Ambient pressure. The solid line is a fit as described in text. Dashed-dotted (dashed) line shows the liquid-like (Lorentzian) component. (b) SRO pattern measured at ambient pressure and under pressure ($P_i=4.6$ GPa, $P_u=0.2$ GPa) in the same q range. Solid lines are fits as described in text.

both the SL behavior and the \mathbf{k}_1 order at the expense of the \mathbf{k}_0 order. To understand this result, one needs to consider the effects of isotropic and uniaxial pressure components separately. An isotropic pressure of 4.6 GPa induces an average compression of the lattice $\Delta V/V$ of about 2%.^{24,25} This favors the SL rather than the \mathbf{k}_0 structure, like under chemical pressure when Sn is replaced with Ti of smaller ionic radius. Compressing the lattice enhances the AF superexchange with

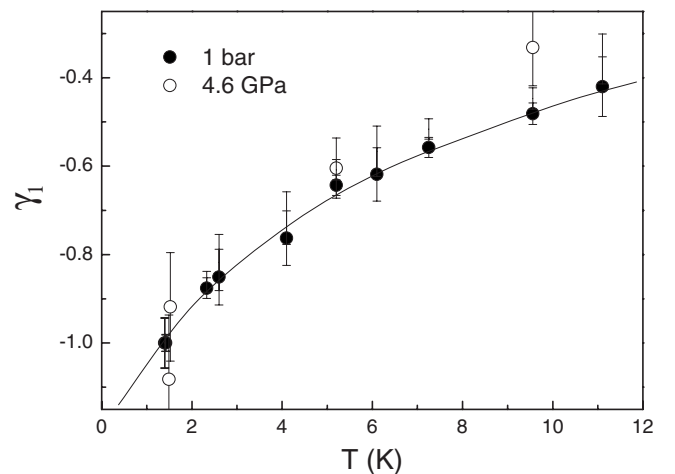


FIG. 4. Temperature dependence of the first-neighbor correlations in the paramagnetic region. Solid line is a guide to the eye.

respect to the F dipolar interaction. The influence of the stress depends on its orientation with respect to the crystal axes, and a powder average must be performed. In TTO single crystal,¹⁵ a stress along a [110] axis induces the \mathbf{k}_1 order with ordered moment at 0.1 K up to $3.9\mu_B$ and T_N of 1.8 K. The [110] stress relieves the geometrical frustration by inducing three different bond lengths in the distorted tetrahedron. This is not the case for stresses along [111] or [100] axis, which have a much smaller effect.

To evaluate the effect of the stress on the powder sample, noticing that the smallest angle between [110] and [111] axes is 35° , we assume that only stresses applied close to a [110] axis can induce the \mathbf{k}_1 order. In a powder sample, the probability of finding a [110]-type axis in a cone of angle θ is simply given by $P(\theta)=6(1-\cos\theta)$, for $\theta\leq 30^\circ$. Taking, for instance, $\theta=20^\circ$, we find that 36% of the grains should experience an efficient stress. We therefore conclude that both SL and \mathbf{k}_1 orders are favored by pressure, but in different ways. With these assumptions, the \mathbf{k}_1 structure occurs only in the well-oriented grains, with a strong moment $M_1=4.7\mu_B$ and a total one of $5.4\mu_B$, whereas in the other grains SL and \mathbf{k}_0 orders are stabilized. This inhomogeneous picture of the pressure-induced ground state also accounts for the different transition temperatures found for both structures.

Our results bring strong evidence that the magnetoelastic coupling responsible for the pressure-induced \mathbf{k}_1 order in TTO is also at play in TSO. The high sensitivity of the magnetic interactions to a pressure-induced distortion allows one to tune ordered spin ice, spin liquid, and AF orders through pressure and stress. This coupling also plays a role at ambi-

ent pressure. In TTO, a spontaneous distortion was observed, likely precursor of a Jahn-Teller transition.²⁶ Recent results²⁷ suggest that this distortion is also present in TSO and helps stabilizing the ordered spin ice state. A quadratic distortion corresponding to an energy scale $D_Q=0.2$ K can account for the canting angle $\alpha=13^\circ$, not explained by the soft spin ice model.²⁰ One naturally expects this distortion to increase under stress. This could explain both the increase in the canting angle in the \mathbf{k}_0 structure (a distortion $D_Q=0.4$ K yields $\alpha=26^\circ$ close to the experimental value) and the onset of the \mathbf{k}_1 structure.

This spin-lattice coupling should be considered both at the local level (the crystal field) and for the collective states. Taking it into account may help one to understand the special properties of terbium pyrochlores, with giant magnetostriction and paraelectric constant, magnetic orders induced by stress or magnetic field applied along $\langle 110 \rangle$ axes only, and spin fluctuations in the ground state.

In conclusion, applying pressure in $\text{Tb}_2\text{Sn}_2\text{O}_7$ soft spin ice destabilizes the ordered spin ice state and induces spin liquid and antiferromagnetic orders. This onset occurs through two different mechanisms, which evidence the effect of isotropic compression on the energy balance of magnetic interactions and the influence of the pressure-induced distortion on the magnetic exchange and crystal field, respectively.

I.M. thanks P. Bonville for communicating unpublished results, and G. André and J. M. Mirebeau for fruitful discussions. H.C. acknowledges support from the Triangle de la Physique.

¹S. Lee *et al.*, Nature (London) **451**, 805 (2008).

²S. Pailhès, X. Fabréges, L. P. Régnault, L. Pinsard-Godart, I. Mirebeau, F. Moussa, M. Hennion, and S. Petit, Phys. Rev. B **79**, 134409 (2009).

³O. Tchernyshyov, R. Moessner, and S. L. Sondhi, Phys. Rev. Lett. **88**, 067203 (2002).

⁴S. T. Bramwell and M. J. P. Gingras, Science **294**, 1495 (2001).

⁵A. P. Ramirez *et al.*, Nature (London) **399**, 333 (1999).

⁶C. Castelnovo, R. Moessner, and S. L. Sondhi, Nature (London) **451**, 42 (2008).

⁷T. Fennel *et al.*, Science **326**, 415 (2009).

⁸L. D. C. Joubert, P. C. W. Holdsworth, and R. Moessner, ESF-HFM Workshop, Abingdon, 2009 (unpublished).

⁹I. Mirebeau and I. N. Goncharenko, Physica B **350**, 250 (2004).

¹⁰M. Mito *et al.*, J. Magn. Magn. Mater. **310**, e432 (2007).

¹¹M. J. P. Gingras, B. C. den Hertog, M. Faucher, J. S. Gardner, S. R. Dunsiger, L. J. Chang, B. D. Gaulin, N. P. Raju, and J. E. Greedan, Phys. Rev. B **62**, 6496 (2000).

¹²I. Mirebeau, P. Bonville, and M. Hennion, Phys. Rev. B **76**, 184436 (2007).

¹³I. V. Alexandrov *et al.*, Sov. Phys. JETP **62**, 1287 (1985).

¹⁴I. Mirebeau, I. N. Goncharenko, S. T. Bramwell, M. J. P. Gingras, and J. S. Gardner, Nature (London) **420**, 54 (2002).

¹⁵I. Mirebeau, I. N. Goncharenko, G. Dhalenne, and A. Revcolevschi, Phys. Rev. Lett. **93**, 187204 (2004).

¹⁶I. Mirebeau, A. Apetrei, J. Rodriguez-Carvajal, P. Bonville, A. Forget, D. Colson, V. Glazkov, J. P. Sanchez, O. Isnard, and E. Suard, Phys. Rev. Lett. **94**, 246402 (2005).

¹⁷F. Bert, P. Mendels, A. Olariu, N. Blanchard, G. Collin, A. Amato, C. Baines, and A. D. Hillier, Phys. Rev. Lett. **97**, 117203 (2006).

¹⁸P. Dalmas de Réotier *et al.*, Phys. Rev. Lett. **96**, 127202 (2006).

¹⁹S. R. Giblin, J. D. M. Champion, H. D. Zhou, C. R. Wiebe, J. S. Gardner, I. Terry, S. Calder, T. Fennell, and S. T. Bramwell, Phys. Rev. Lett. **101**, 237201 (2008).

²⁰J. D. M. Champion, S. T. Bramwell, P. C. W. Holdsworth, and M. J. Harris, EPL **57**, 93 (2002).

²¹I. N. Goncharenko, High Press. Res. **24**, 193 (2004).

²²E. F. Bertaut, Acta Crystallogr., Sect. A: Cryst. Phys., Diffr., Theor. Gen. Crystallogr. **24**, 217 (1968).

²³J. S. Gardner *et al.*, Phys. Rev. Lett. **82**, 1012 (1999).

²⁴R. S. Kumar *et al.*, Appl. Phys. Lett. **88**, 031903 (2006).

²⁵A. Apetrei, I. Mirebeau, I. Goncharenko, and W. Crichton, J. Phys.: Condens. Matter **19**, 376208 (2007).

²⁶J. P. C. Ruff, B. D. Gaulin, J. P. Castellán, K. C. Rule, J. P. Clancy, J. Rodriguez, and H. A. Dabkowska, Phys. Rev. Lett. **99**, 237202 (2007).

²⁷K. C. Rule and P. Bonville, J. Phys.: Conf. Ser. **145**, 012027 (2009); P. Bonville *et al.* (unpublished).